climate

MDPI

Article

Resilience of the North Atlantic Circulation on Decadal Timescales

Dan Seidov [1], Alexey Mishonov [1,2,*] and James Reagan [1]

[1] National Centers for Environmental Information, NOAA, SSMC3, 1315 East-West Hwy, Silver Spring, MD 20910, USA
[2] Cooperative Institute for Satellite Earth System Studies, University of Maryland, 5825 University Research Ct, College Park, MD 20740, USA
* Correspondence: alexey.mishonov@noaa.gov

Abstract

The circulation of the North Atlantic Ocean plays a vital role in the Earth's climate system. Numerous studies, primarily through computer simulations, have examined the stability of the Atlantic Meridional Overturning Circulation (AMOC) in a warming climate. Some of these studies predict a potential collapse of the AMOC in the foreseeable future, which would require a significant influx of freshwater into the subpolar North Atlantic (NA) and Nordic Seas. Paleoreconstructions of NA circulation indicate a major shift in the position of the subpolar cold front, which either precedes or coincides with substantial changes in AMOC dynamics. These changes in the front position imply a significant alteration in circulation patterns, beginning with the noticeable restructuring of the subtropical and subpolar gyres. This would lead to modifications in the Gulf Stream system and the North Atlantic Current (NAC), affecting the thermohaline fields and the position and strength of these two current systems. Although some models predict a significant slowdown or even collapse of the AMOC, recent observational studies have offered a more cautious perspective. For instance, the Gulf Stream system exhibits high resilience to perturbations caused by ongoing sea surface warming. In this study, we analyzed the decadal variability of temperature and salinity from in situ observations, along with upper-ocean currents in the subpolar NA (SPNA). We found that the thermohaline pattern of the upper ocean layers in the SPNA and Nordic Seas has remained resilient for over 70 years. The deceleration of the AMOC is evident but relatively modest, with average velocities in the upper layers decreasing by less than 10–15% over 30 years. This deceleration was also inconsistent throughout the NAC region. Furthermore, the subpolar front migration over 70 years, as manifested in isotherm spatial variability, reached a maximum of 3° of latitude, with spatial variability of the yearly 10 °C isotherms being lower. Overall, the conclusion regarding the resilience of the NAC aligns well with that of the Gulf Stream, with no substantial changes in the position or intensity of the subpolar gyre. We conclude that while the AMOC is susceptible to some deceleration due to ongoing surface warming and/or high-latitude freshening, it may also be sufficiently resilient to withstand these changes. Although it cannot be entirely ruled out that the AMOC may reach its tipping point within this century, an analysis of data on decadal variability in the upper arm of the AMOC suggests that such a collapse is unlikely to occur.

Keywords: North Atlantic Ocean circulation; ocean variability; climate change; Gulf Stream system; Atlantic Meridional Overturning Circulation (AMOC)

Academic Editors: Mengrong Ding and Aixue Hu

Received: 15 April 2026
Revised: 30 April 2026
Accepted: 30 April 2026
Published: 2 May 2026

1. Introduction

The North Atlantic (NA) Ocean is a vital component of ocean-atmosphere interactions and is a key driver of regional and global climates. Central to the North Atlantic circulation is the Atlantic Meridional Overturning Circulation (AMOC), which powers the entire global conveyor. It is believed that the climate is so reliant on the AMOC that any significant alteration could drastically impact the global thermohaline circulation, also known as the global ocean conveyor belt, and consequently, the global climate (see, for example, [1,2]). Some studies have predicted that the AMOC may collapse in the foreseeable future, e.g., [3–5]. Some authors argue that the AMOC may be nearing its tipping point in the foreseeable future if global warming reaches a certain threshold (see a detailed discussion of the AMOC as a tipping point in [6]). While some models predict severe changes in the AMOC, others suggest more moderate scenarios [7] (see discussion in [8]). A new study by [9] infers, based on air–sea heat flux analysis, that the decadal-average AMOC at 26.5° N did not weaken from 1963 to 2017, although some noticeable variability occurred at all latitudes in other time periods. Moreover, based on various numerical studies, the IPCC states that an AMOC collapse is unlikely to occur in the near future [10]. The essence of this issue is that the scenarios generated by the model simulations exhibit excessive variation.

Many predictions of severe AMOC alteration or even collapse require a substantial influx of Arctic freshwater into the Subpolar North Atlantic (SPNA) and Nordic Seas (NORS). In many numerical experiments using both standalone ocean models and sophisticated climate models, the AMOC slowdown or potential collapse is driven by the continuous influx of meltwater into these regions, leading to a more stable water column and a reduced deep-water formation. A substantial amount of freshwater can diminish the sea surface salinity (SSS) in these regions by more than 1 psu, which is approximately 3% of the typical salinity in the North Atlantic (~34 psu). (Although salinity is a dimensionless variable, discussing its deviations makes using dimensionless numbers somewhat awkward. Therefore, we use practical salinity units (psu) to enhance the text's flow.) Significant reductions in the AMOC were evident in these simulations only when salinity changes were large (see the discussion in [11]). Recent modeling studies indicate that, under such circumstances, the AMOC could reach its tipping point, and the entire climate system would respond accordingly. The question is whether the current sea surface salinity trends meet these requirements.

According to most numerical simulations, this substantial freshwater influx is expected to be localized in the NORS and SPNA, especially in the Irminger Sea, which can be considered the epicenter of AMOC driving, e.g., [12,13]; see also a review in [11]. Even a cursory examination of in situ observations and NA decadal climatologies, for example, from NOAA's World Ocean Atlas (WOA), does not corroborate the sea surface salinity (SSS) trends that would lead to such significant freshening in these regions [14]. Additionally, while much of the NA sea surface is warming, trends in sea surface temperature (SST) have not been significant over the last several decades. Furthermore, reconstructions of NA circulation over the past 150 years indicate that a major shift in the position of the subpolar cold front preceded or coincided with a substantial change in the AMOC [15]. These changes suggest a significant alteration in the circulation pattern, beginning with a noticeable restructuring of the subtropical and subpolar gyres.

The cold subpolar front is a specific feature of the SPNA that may be indicative of the tendencies of the AMOC and the overall horizontal and vertical circulation in this region. The cold subpolar front in the North Atlantic is a region of sharp temperature gradients that marks the boundary between the subtropical and subpolar gyres. It is located south of Greenland and extends eastward, approximately within the 50° N–60° N latitude band. This can be associated with the 10 °C isotherm, which runs along the boundary between the subtropical and subpolar gyres, e.g., [16–18].

The location and orientation of the subpolar front are linked to the strength of the AMOC. During the Last Glacial Maximum (LGM, approximately 21–18 thousand years ago, i.e., 21–18 Kya), for example, [19], the subpolar front stretched longitudinally across the North Atlantic at ~40° N, which capped the northern extent of the North Atlantic Current and was associated with cold conditions and a weak AMOC (see Figure 1 in [11]). However, during the Holocene period (present day), the North Atlantic subpolar front is oriented from southwest to northeast, allowing warmer subtropical waters to penetrate into the high latitudes, which in turn yields a stronger AMOC and warmer temperatures (e.g., [19]).

The AMOC has undergone significant changes since the last deglaciation (see, for example, [20,21]). Some authors have argued that the subtropical NA gyre was deeper and stronger during the LGM than today, e.g., [22]. Similarly, ref. [23] noted that the upper-ocean wind-driven subtropical gyre during the LGM was more potent than the present-day circulation. A shift in the orientation of the subpolar front was also observed in this study. The progression of the subpolar front has been discussed in various publications, for example, [19,24–29].

Future sea surface temperatures may be warmer than today in the SPNA and NORS if the ongoing warming continues, causing a substantial change in SST (and presumably SSS) patterns and a noticeable reorientation of the NAC and the subpolar front. The latter has not been observed in thermohaline in situ data, at least not during the last six decades. It has been shown that the Gulf Stream remains highly resilient to the ongoing warming of the NA surface and that its axis remains stable with minimal shifts [30]. Moreover, a recent study by [31] showed that the annually averaged changes in NA circulation were noticeable but not excessive and that the gyres' boundaries did not change. In contrast, the AMOC collapse paradigm suggests severe changes that would push the system beyond the AMOC tipping point.

We investigated changes in the thermohaline fields in the SPNA and Nordic Seas over the last 60+ years using in situ temperature and salinity data from the World Ocean Database (WOD) [32] and analyzed the fields from the World Ocean Atlas 2023 (WOA23) [14,33]. Decadal density was derived from WOA23, while annual density was calculated using the Ocean Data View (ODV) program [34], based on in situ temperature and salinity data from WOD for the period from 1955 to the latest WOD update (2025 Q2), and sea surface height (SSH) and wind stress from the SODA3 project [35].

2. Previous Data Analyses

To recap, we briefly summarize the findings of [30,31], as the methods and data structures we employ closely resemble those used in these two studies. We also refer readers to a recent review that summarizes these findings and compares NA variability from modeling and observational perspectives [11].

In their 2019 study [30], the authors mapped the annual and decadal positions of the 15 °C isotherm at a depth of 200 m across the region spanning 80° W–40° W and 30° N–50° N using data from the World Ocean Database 2018 (WOD18). They discovered that the Gulf Stream path remained notably stable between approximately 75° W and 50° W, a region referred to as the "robust zone." However, east of approximately 50° W, in what is known as the Gulf Stream "extension zone," the Gulf Stream Cold Wall (GSCW) exhibited greater variability and a more pronounced northward drift, reaching up to ~2.6° latitude over ~50 years in certain sections, whereas the robust zone experienced only a ~0.4° latitude shift during the same period. Notably, the changes in the Gulf Stream path (including the extension zone) were not substantial (see details in [30]). This study highlights the surprising rigidity of the Gulf Stream, with an essentially unchanged subsurface GSCW between Cape Hatteras and approximately 50° W, in contrast to a more mobile and variable

eastward extension that has migrated significantly northward over the past 50 years. Ocean heat content within the upper 700 m layer of the ocean emerged as the strongest variable associated with these decadal changes, indicating that interior ocean warming plays a crucial role in controlling the Gulf Stream pathway over long timescales. The analysis in this study does not suggest any dramatic changes in the upper arm of the AMOC in the coming decades. In this study, we focused mostly on the SPNA and NORS, with special attention to the Irminger Sea and surrounding waters.

Mishonov and co-authors [31] expanded on previous analyses of the North Atlantic's decadal variability in the upper-ocean temperature field by incorporating factors such as salinity, density, and the geometry of wind-stress curl and Ekman pumping. They found that recent decadal changes in the upper-ocean circulation of the North Atlantic were driven by thermohaline processes rather than by significant changes in the geometry of wind-driven gyres. Additionally, they noted a moderate deceleration of the AMOC but no substantial changes in the structure of water transport or thermohaline field over the past three decades.

3. Data and Methods

To assess the actual changes in temperature and salinity within the subsurface layers of the SPNA, we examined decadal-averaged temperature maps for winter, summer, and the yearly average over the past five decades: 1975–1984, 1985–1994, 1995–2004, 2005–2014, and 2015–2022. The baseline NA ocean climate from WOA is the 30-year temperature and salinity averaged over the three decades 1985–1994, 1995–2004, and 2005–2014, and it is considered the mean state (this time interval is the closest to U.S. climate normals of 1991–2020). It is important to note that the last "decade" is two years short of a full decade, as the data published in WOD23 and WOA23 conclude in 2022; however, for consistency, we still refer to it as a decade. The latest WOD update, at the time of writing (Q2 2025), was utilized to determine the yearly positions of isotherms, isohalines, and isopycnals, as well as to compute the time series of anomalies for these variables. Additionally, we used sea surface elevation data from the Simple Ocean Data Assimilation version 3 reanalysis product (SODA3) [35] for the three decades 1985–1994, 1995–2004, and 2005–2014. We opted for SODA v3.4.2 because it effectively reduces the systematic errors found in SODA v2 [35] and is driven by the ERA-I atmospheric reanalysis, which provides higher-quality and higher-resolution surface forcing than the CR20v2 forcing used by SODA v2. Additionally, SODA v3.4.2 uses a more recent version of the WOD, with 40% more ocean profiles than SODA v2. Consequently, we chose the more accurate reanalysis over a less precise one with a longer time span.

The decadal-averaged sea surface elevations from SODA3 were combined with the density from WOA18 to compute geostrophic velocities in the upper 1.5 km of the ocean. These were then evaluated to document changes in currents and water transport variability over the last three decades (details are available in [31]). The winter, summer, and annual strengths of the currents in the upper 500 m of the region were mapped and investigated.

That is, the wind stress and sea surface elevation were obtained from SODA3, while the yearly, annual, and seasonal temperature, salinity, and density were obtained from the WOD, and the decadal climatological values of these variables were obtained from the WOA. The yearly positions of several selected isotherms in the SPNA and NORS were calculated for the winter and summer seasons, and their annual positions were determined to assess their migration over the last 60+ years.

4. Results

We begin by examining the differences in winter decadal temperature, salinity, and density. Our primary focus was on the winter season because deep-water formation in the SPNA and NORS is seasonal and most pronounced then. Figure 1 illustrates the winter differences in temperature, salinity, and density between the most recent decade of 2015–2022 and the earliest decade of 1985–1994 in the selected sequence of the analyzed fields at 50 m depth. These two decades were chosen to examine the most recent changes in *decadal* climatology, utilizing the velocity calculated using surface elevation data from SODA3, as well as temperature and salinity data from WOA. Additionally, this period aligns with both modeling efforts to simulate AMOC-impacting meltwater pulses (see a review in [11]) and data-based monitoring of the AMOC that commenced in the first two decades of the 21st century, e.g., [36–38]. The differences were noticeable but not substantial. Temperature variations ranged from 3 °C to −0.5 °C, and salinity differences ranged from 1.0 to −0.5 psu (with the greatest differences in the core GS area). The density changed from 0.4 to −0.5 kg m^{-3}, with much of the region in the range ±0.2 kg m^{-3}, which is very small compared to the average density of the global ocean (~1025 kg m^{-3}).

The initial examination of the thermohaline structure suggested that the temperature, salinity, and density differences were not substantial (not exceeding 3 °C, 0.9 psu, and 1 kg m^{-3}, respectively; see above). However, the pattern of these differences makes it difficult to determine the structural changes. Contrary to what could be the driver of the AMOC weakening, which would be a substantial freshening of the SPNA and NORS, there was no definitive salinity reduction in the surface layer in the SPNA and only a subtle decrease in the NORS. However, near-surface temperatures have increased almost everywhere. This ongoing warming in the North Atlantic has been well documented (e.g., [39]). It is also true that the upper-layer water became lighter (i.e., less dense) over the period from 1985 to 2022 (Figure 1c). However, the regions with the largest near-surface density decrease are not in deep-water formation locales (e.g., the SPNA and NORS). In fact, the SPNA and NORS experienced some of the weakest density decreases (0 to −0.1 kg m^{-3}) across NA. These small changes are not large enough to reduce the AMOC, let alone push it past its tipping point.

Figure 1 highlights the winter differences because, as mentioned before, deep-water formation in the SPNA and NORS is seasonal and peaks in winter. Analysis of summer fields revealed even more modest decadal contrasts than those in winter. Consequently, we omitted showing the summer and annual differences, as they do not provide additional insights beyond those offered by the winter data.

In Figure 1a, two rectangles—one located in the eastern SPNA (Region 1, labeled *R1*) and the other in the NORS (Region 2, labeled *R2*)—highlight the areas where the area-averaged temperature, salinity, and density at various depths were calculated. Because the precise location of deep-water formation in the SPNA and NORS cannot be determined annually for every year, the boxes in Figure 1a are not intended to depict the exact deep-water formation zones. Instead, they were selected to represent areas that approximately converged in these zones. This approach was used to illustrate the trends of these parameters using in situ data from the WOD over roughly seven decades. It is important to note that the standard deviation or standard error of the mean is only applicable when data are available. However, this region was extensively sampled, and the standard errors of the means were significantly smaller than the resulting decadal differences. The standard errors of the mean for decadal climatology arrays are available on the WOA website.

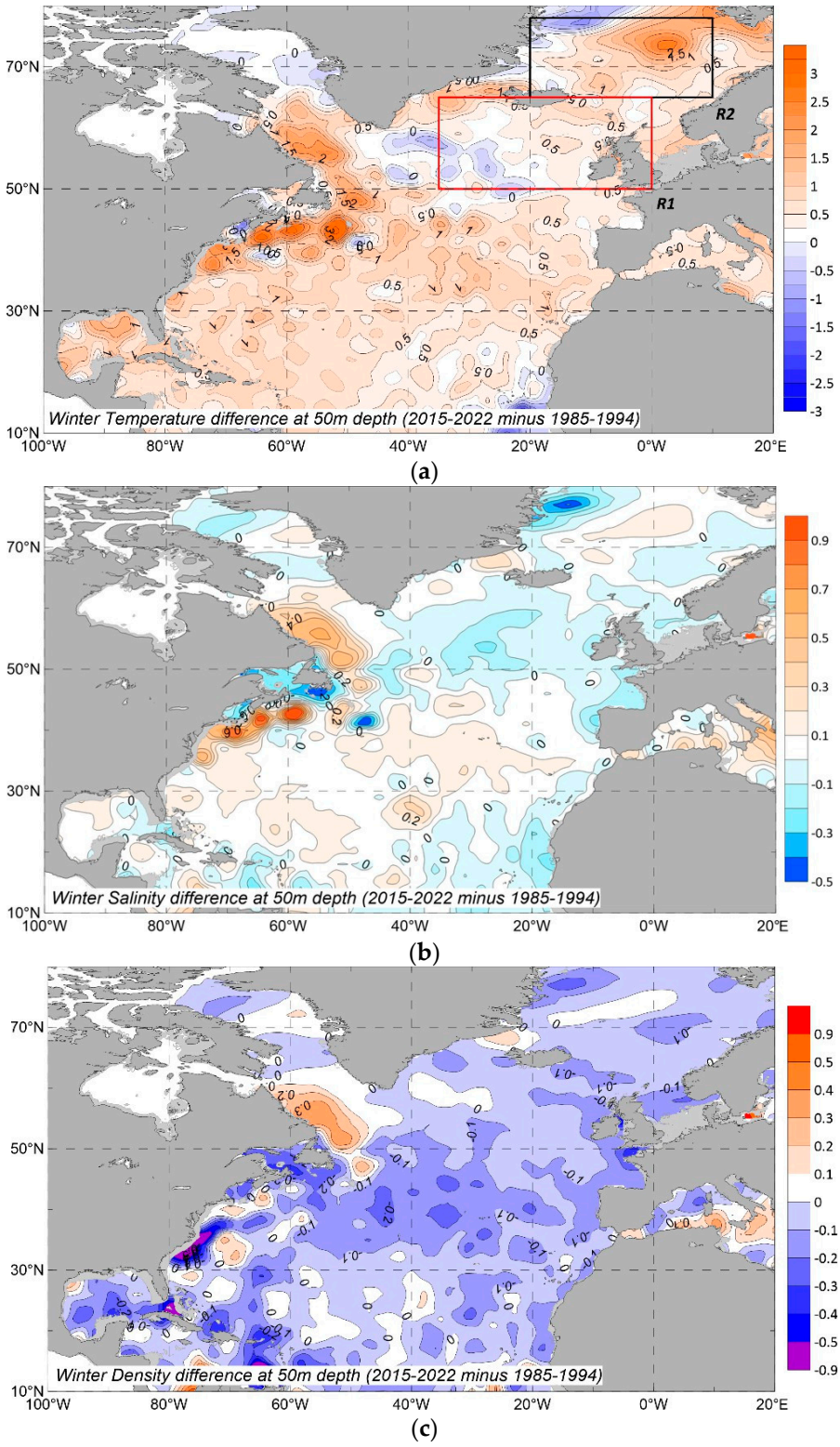

Figure 1. Differences in winter sea water temperature (**a**), salinity (**b**), and density (**c**) at 50 m depth between 2015−2022 and 1985−1994 decades (based on WOA23). The red and black rectangles in (**a**) delineate the boxes in which a series of area-averaged annual temperature, salinity, and density were analyzed (see text).

The temperature variations south and southwest of Greenland highlight the warming hole (or "cold blob") that has been extensively discussed in numerous publications examining temperature changes in the North Atlantic over the past century and the first two decades of this century, e.g., [6,38,40–42] (further details in [10]). This phenomenon is

thought to be linked to the ongoing weakening of the AMOC, which has been monitored since 2004 [36]. However, the relative cooling of the central part of the SPNA began well before the launch of direct AMOC monitoring. Reports indicate that the warming hole has evolved over at least the past 70 years [40–42]. Seidov et al. [43] compared ocean heat content across two 30-year climatologies from WOA, uncovering significant cooling in the upper layers southwest of Greenland between 1985 and 2012 and 1955 and 1984, while other regions experienced warming. Additionally, some researchers have observed notable freshening of the sea surface in this area [40–42]. Our findings corroborate these analyses, with Figure 1b clearly showing substantial freshening, as indicated by the blue areas. For instance, similar to the sea surface salinity trends highlighted in [40,42], significant salinization occurred in the Gulf Stream region and in the western Labrador Sea, along with notable freshening in the central SPNA, south and southeast of Greenland.

The differences in climatology were determined using decadal climatologies from WOA, whereas the yearly positions of the isotherms, isohalines, and isopycnals were calculated using all data from WOD (1955 through the second quarter of 2025). The annual time series for density, as illustrated in Figure 2, was calculated using the WOD data. Using climatological data from the WOA would result in too few time points in the series, and it would be impossible to generate spaghetti envelopes for the positions of temperature and salinity (Figure 3).

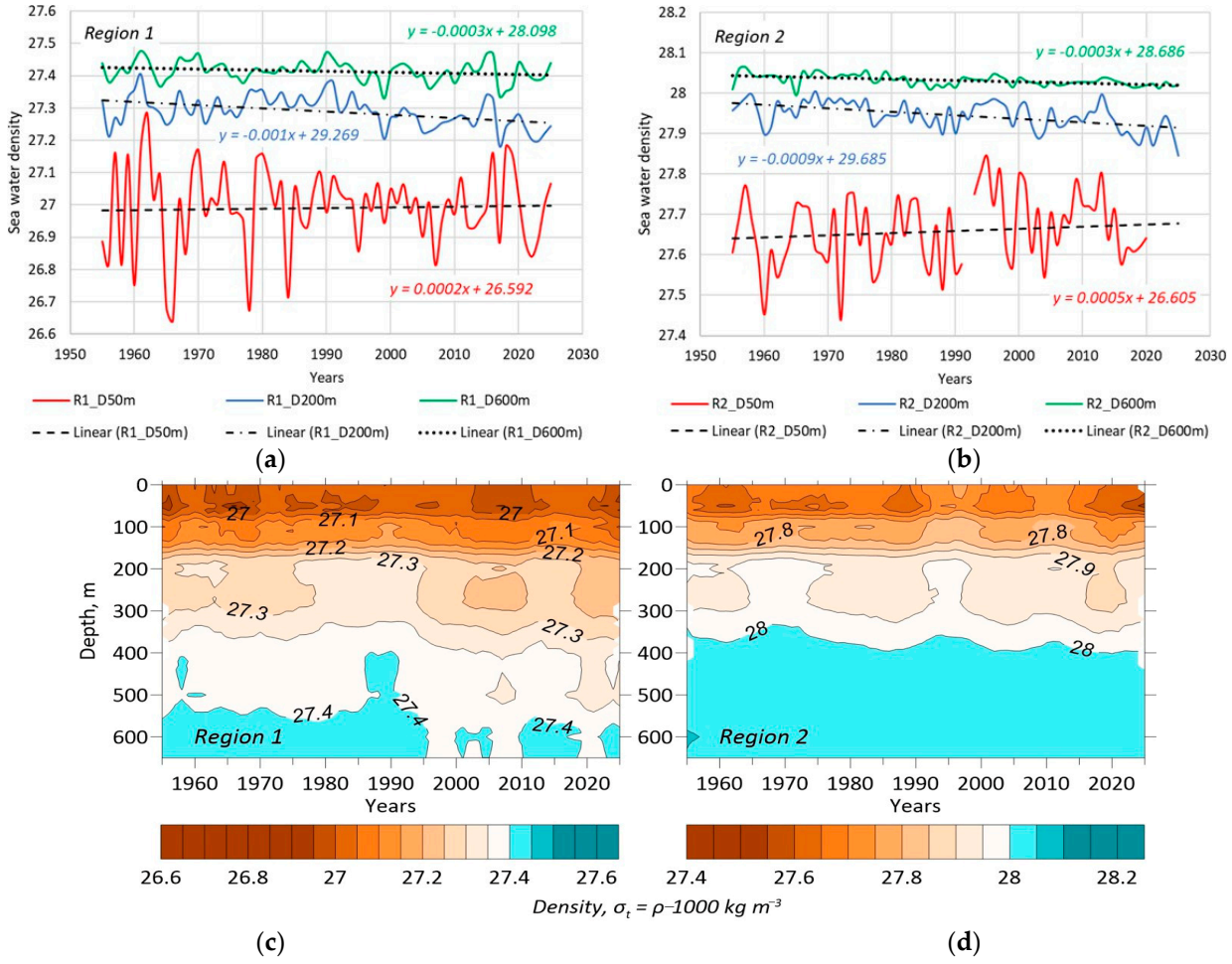

Figure 2. Annual density time series averaged over *R1* and *R2* areas (see Figure 2a) at 50 m (red lines), 200 m (blue lines), and 600 m (green lines) depths in region 1 (**a**) and region 2 (**b**); linear trend lines also shown. Hovmöller diagrams of the density–depth evolution in region 1 (**c**) and region 2 (**d**). The density is $\sigma_t = \rho - 1000$ kg m^{-3}.

Table 1. The position of the 70-year averaged annual 10 °C isotherm at two locations in the SPNA shown in Figure 3a, as well as the standard deviation of the yearly positions of these isotherms at 50 m and 200 m.

Depth	50 m	200 m
Mean 10 °C position at 30° W	53.05° N	49.85° N
STD at 30° W	3.44° of latitude	1.31° of latitude
Mean 10 °C position at 20° W	58.10° N	54.99° N
STD at 20° W	3.07° of latitude	2.79° of latitude

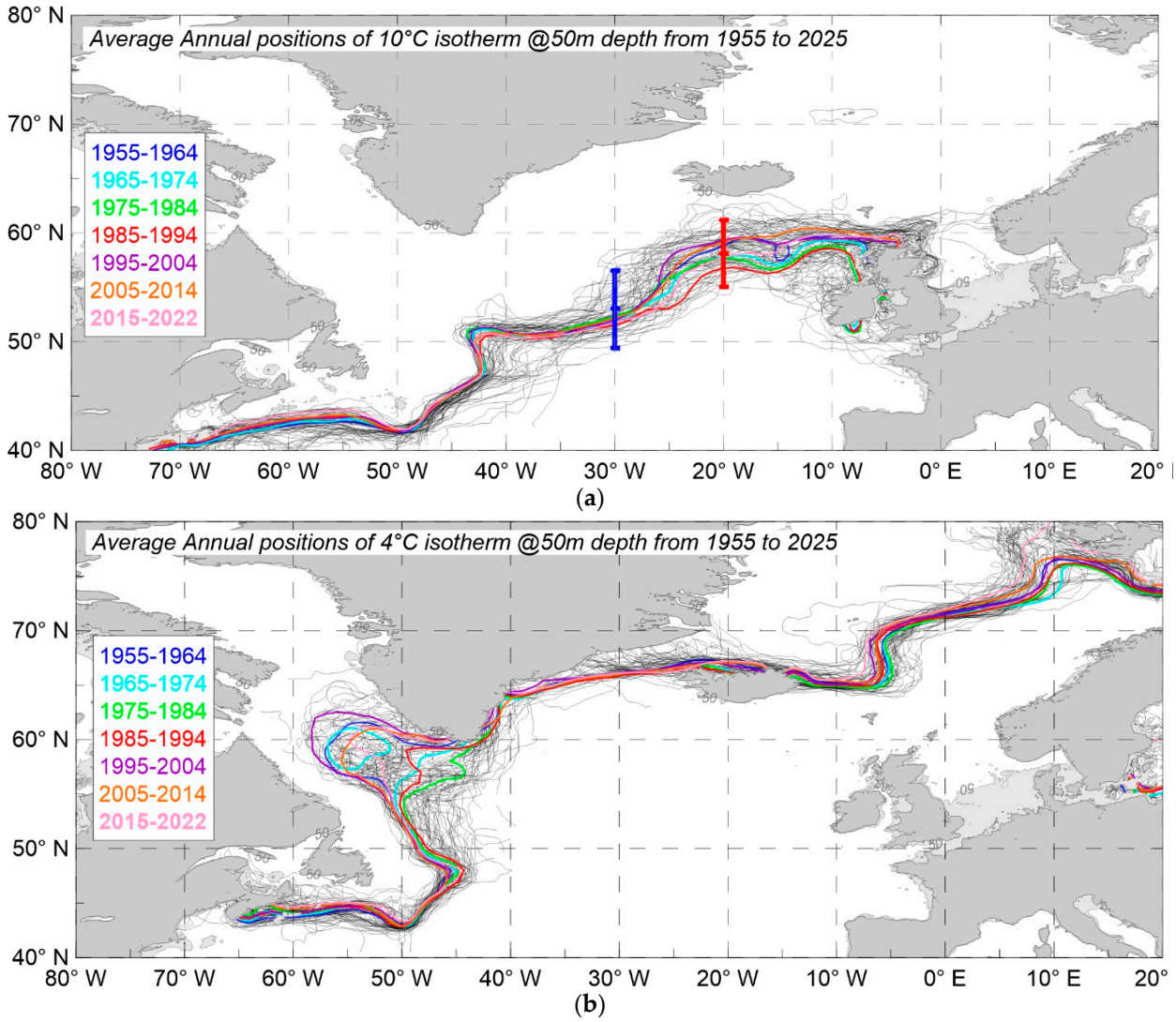

Figure 3. Annual positions of 10 °C (**a**) and 4 °C (**b**) isotherms at 50 m depth from 1955 to 2025. Based on observational data from the WOD (2025-Q2 update). The decadal-averaged positions of these isotherms for the seven decades from 1955 to 2022 are shown as bold-colored lines (based on the WOA23). Two sections on (**a**) across the 10 °C spaghetti at 30° W (blue) and 20° W (red) indicate the locations where the standard deviation of the individual annual 10 °C isotherm positions was calculated (Table 1).

The area-averaged temperature and salinity showed slight trends in both regions. These changes pale in comparison to the many numerical model simulations of meltwater impact in the high latitudes of the NA, where, for example, changes of 1.0 over 100 years were implemented. Such significant freshening of the upper layers could have occurred

in the geological past and is thus justified in some models, for example, [23], but modern trends do not support such intense freshening, which could have caused an AMOC collapse.

Recognizing the critical role of the vertical density gradient in deep-water formation and AMOC functioning, we focused solely on density trends. Figure 2 displays the area-averaged annual density for region 1 (a) and region 2 (b) at 50 m, 200 m, and 600 m depths. Notably, the density at 50 m indicates a slight increase in the surface layer density, while at 200 m and 600 m, the density shows a slight decrease (linear trend lines in Figure 2a,b). This suggests an overall decrease in the vertical hydrostatic stability in the subsurface layers of both regions.

As vertical stability increases, deep-water production may decline over time, potentially explaining the modest slowdown of the AMOC, particularly because the density decrease in the upper layers of the NORS is more pronounced. Conversely, if vertical stability decreases, the AMOC might accelerate, as illustrated in Figure 2 by comparing 50 m and 200 m. However, the density at 600 m in both regions decreased at a slightly slower rate than at 200 m, indicating that vertical stability increased with depth. This could potentially result in a reduction in deep-water formation, confining increased convection to the upper layers alone. Nonetheless, the minimal changes in vertical stability indicate a moderate alteration in deep convection, which does not support any conclusions about a significant AMOC response.

The Hovmöller diagrams in Figure 2c,d show the temporal stability of the density profiles. In region 1, subtle year-to-year variations in stratification were observed in the upper layers (above 300 m), with a slight downward reduction in density below 300 m. While the density in the upper 50 m revealed significant annual variability (red lines in Figure 2a,b), the 70-year average density in this layer remained largely stable in the SPNA but showed modest densification in the NORS. Overall, the density progression in both regions suggests modest changes in the density profiles and, consequently, in the vertical stability of the water columns in these regions. Densification of the subsurface layer in the NORS may suggest that this layer is becoming more stable as the SPNA and NORS climates evolve. Whether this would be sufficient to slow the AMOC is beyond the scope of this presentation.

The next series of results analyzed the critical frontal lines associated with the cold subpolar front and the incursion of NA water into the NORS. The 10 °C isotherm at 50 m depth (that is within the subsurface mixed layer) is commonly associated with the subpolar front and the NAC flowing through the eastern part of the SPNA, e.g., [16–18]. The 4 °C isotherm at 50 m depth, along with an SSS of approximately 34.9, serves as a precursor to the formation of North Atlantic Deep Water (NADW) in the SPNA and NORS (see more discussion in [11]). The approach used for plotting the front position was similar to that used in [30].

Figure 3 illustrates the pattern of the annual ensemble of isotherms from 1955 to 2025 based on comprehensive in situ temperature data from the WOD (2025-Q2 update). The figure shows the yearly positions of the 10 °C (a) and 4 °C (b) isotherms at 50 m depth. The cold frontal zone, usually associated with a 10 °C isotherm, is believed to be linked to the NAC and circulation patterns in the SPNA and NORS, e.g., [17,18,44]. As previously mentioned, the 10 °C isotherm is typically associated with the subpolar front in the SPNA, and the 4 °C isotherm (along with salinity values of ~34.9) serves as a precursor to the formation of NADW in the SPNA and NORS. NADW is formed when water cools from the cold atmosphere, becoming dense enough to sink to depth. The yearly isotherms are depicted in gray, whereas the average positions for each of the seven decades from 1955 to 2022 are highlighted in different colors.

The coherence of the position of the 10 °C isotherms at 50 m depth (and similarly at 200 m; not shown) implies that the upper-layer frontal zone is an analog of the Gulf Stream cold wall and a vertical boundary separating warm and cold regions in the eastern SPNA. Table 1 presents the mean geographical positions of the 10 °C isotherm at 50 m depth, along with the standard deviations of its annual positions relative to the 70-year average at 30° W and 20° W longitudes.

Surprisingly, Figure 3b shows that the most significant thermal variability in the surface layer occurred at the 4 °C isotherm in the Labrador Sea. This finding aligns with [30], who found that the Gulf Stream's position showed the greatest variability in the Gulf Stream extension zone adjacent to the cold waters of the Labrador Sea.

In the eastern regions of the SPNA and NORS, the spread of the 4 °C isotherm envelopes was notably less pronounced than that in the western part of the SPNA, especially in the Labrador Sea. Obviously, this depends on the isotherm considered. For example, the 4 °C isotherms exhibited a wider spread in the western SPNA than the 10 °C isotherms, which were very coherent. If AMOC's variability is primarily governed by NADW production in the Labrador Sea, then the large spread of the 4 °C isotherms at the sea surface in the Labrador Sea could have a substantial effect on deep-water production migration in this area. Some authors argue that deep-water production in the Irminger Sea and NORS is the primary driver of the AMOC [12,13], with deep-water formation in the Labrador Sea being the secondary driver. To maintain an unbiased perspective on the relative significance of different deep-water formation zones, we highlight that our research reveals notable variability in the Labrador Sea, which may affect overall deep-water formation in this area.

Figure 4a illustrates the average decadal positions of the 34.9 isohaline, which, at a temperature of 4 °C, may serve as a precursor to NADW formation in the SPNA and NORS (e.g., [45]). Figure 4b depicts the isopycnal ρ = 1027.7 kg m^{-3} (σ_t = 27.70), which is believed to fall within the typical range for the NADW formation. Generally, the isohalines and isopycnals confirmed the resilience of the NAC and subpolar front to ongoing sea surface warming, as they did not significantly migrate, contract, or expand on decadal timescales.

Figure 4a clearly illustrates that the 34.9 psu isohaline, a precursor requirement for NADW formation, remains stable over decadal periods almost everywhere, except in two zones: one southeast of Greenland and the other in the northeast region of the NORS. In all other areas, the isohalines at 34.9 psu and temperatures near 4 °C were largely collinear, as expected, and are characteristic of most parts of the Irminger Sea and NORS. Moreover, the density in these two areas, as shown in Figure 4b, indicates that the western part of the Irminger Sea in winter is preconditioned for deep-water convection. Interestingly, the isopycnals of higher density, specifically 1027.8 and 1027.9 kg m^{-3} (not shown), were generally isolated to the NORS region and therefore had greater surface density than the surrounding regions. Furthermore, in recent decades, the regions in the Labrador and western Irminger Seas with densities exceeding 1027.7 have decreased compared to earlier periods, suggesting a potential reduction in deep-water formation in these areas. This finding challenges the prevailing view that the SPNA and NORS work in unison to sustain the AMOC, as the large area of higher density in the NORS suggests that the NORS is at least as important as the eastern SPNA for controlling the AMOC.

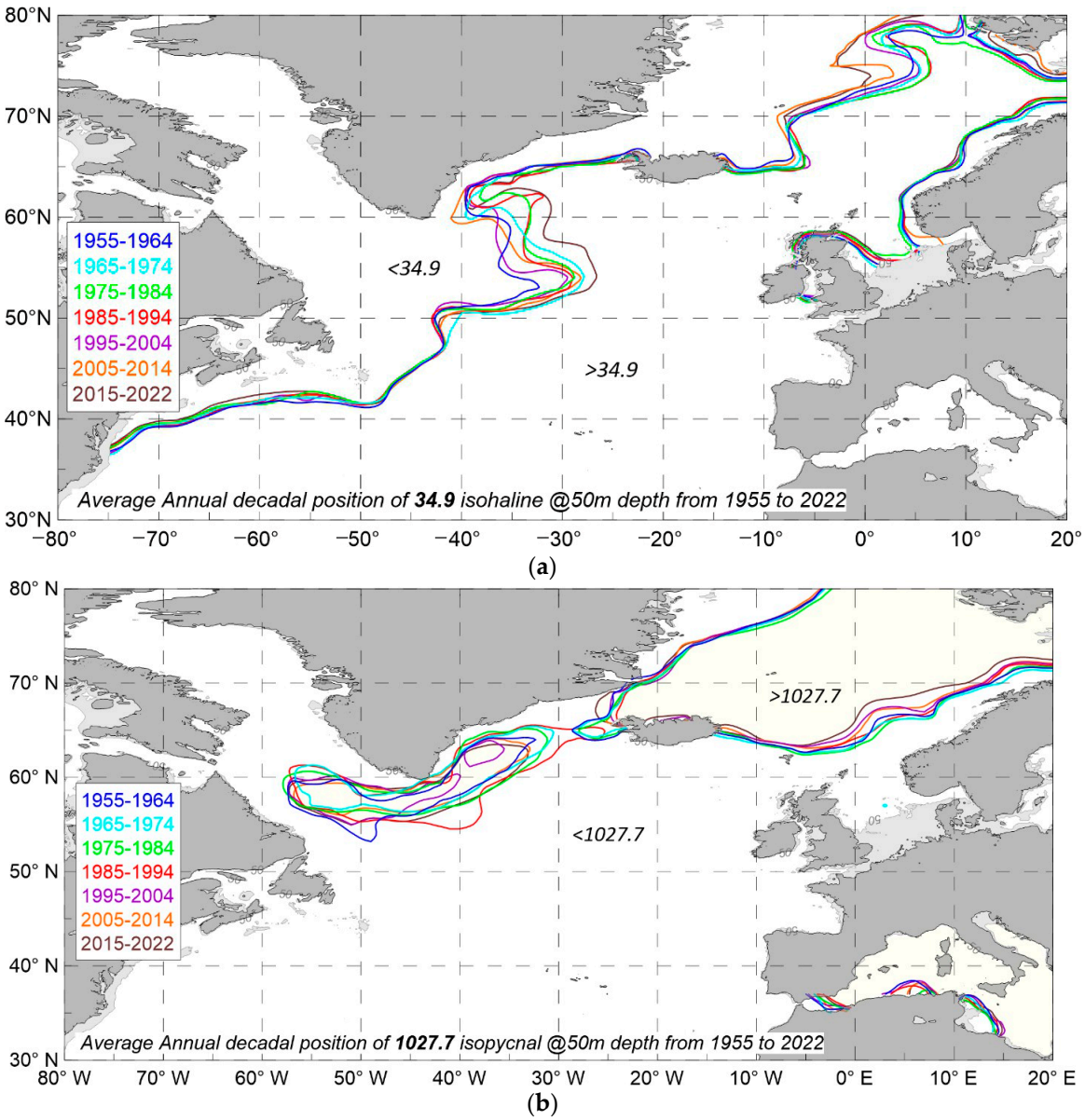

Figure 4. Position of the annual decadal-averaged isohalines of 34.9 psu (**a**) and isopycnals of 1027.7 kg m^{-3} (**b**) at 50 m depth for seven decades from 1955–1964 to 2015–2022 (based on WOA23).

The thermohaline structures of the SPNA and NORS, as revealed by observational data collected over seven decades, suggest that the migration of the critical frontal zones in these regions has not undergone dramatic changes. The observed changes differ significantly from those occurring during glacial–interglacial transformations, as reconstructed using paleo-proxies. For instance, a recent study [46] showed that earlier reconstructions of the Last Glacial Maximum, along with subsequent transitions from cold to warm periods—interrupted by cold spikes and warm episodes coinciding with significant meltwater events—suggest much larger meltwater episodes, potentially leading to dramatic AMOC changes. These events are considered analogs of potential future meltwater episodes that could disrupt the AMOC dynamics. However, these significant meltwater events of the past that could have led to severe changes in the AMOC are much greater than anything observed in the NA over the past 70 years.

Figure 5 illustrates the summer (a) and winter (b) positions of the 1027.7 kg m^{-3} isopycnal with areas of higher and lower density, roughly outlining the potential deep-water formation zones. Although the seasonal migration of isopycnals is substantial,

there is no evidence of significant decadal changes in density during either winter or summer and thus annually (see Figure 4b). While deep water could form sporadically in the northern SPNA and the Labrador Sea during summer, the only region where deep water could (though not necessarily would) consistently form in summer is confined to the NORS. Based on in situ data analysis, we cannot definitively argue for or against specific deep-water formation sites. Furthermore, the isopycnals in Figure 5 were derived from the WOA23, where a vertical adjustment procedure was employed to eliminate vertical instability, which is a crucial factor in deep-water formation. The densities shown in Figure 5 were affected by deep-water formation and vertical mixing, which may have occurred, working to restore the vertical stability of the water columns.

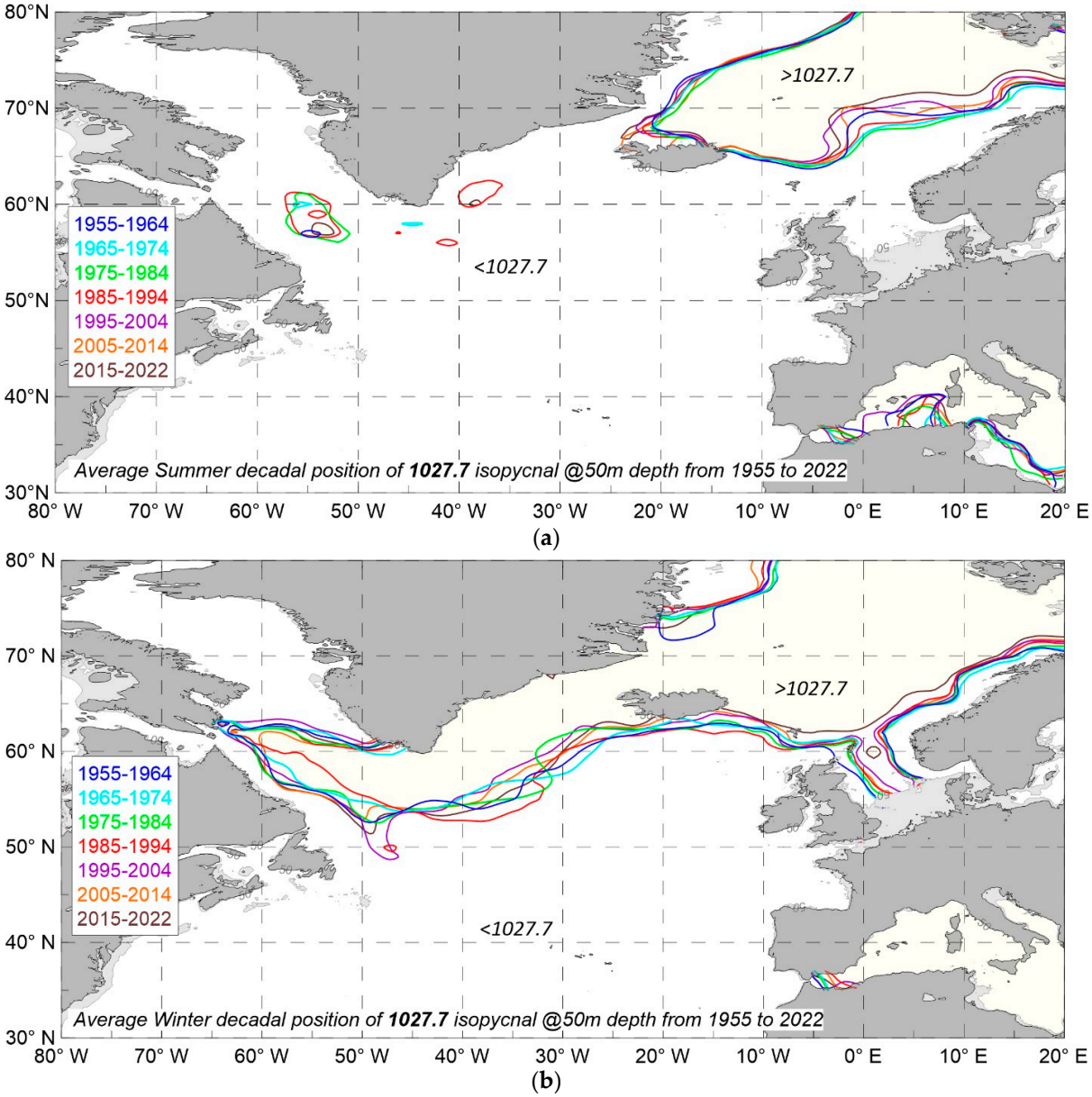

Figure 5. Decadal averaged seasonal isopycnals ρ = 1027.7 kg m^{-3} in summer (**a**) and winter (**b**) at 50 m depth for seven decades from 1955–1964 to 2015–2022 (based on WOA23).

In contrast, the spaghetti plots of temperature in Figure 3 are based on in situ data extracted from the WOD and do not include any vertical adjustment to eliminate hydrostatic instability, which is used when computing the analyzed temperature and salinity climatology fields of WOA23. Nonetheless, our primary focus was the decadal variability

of the thermohaline fields, which may indicate changes that are significant enough to cause a notable decline in the AMOC. Although there were some shifts in the subpolar front position in the eastern SPNA and the incursion of warm and salty Atlantic water in the NORS, these changes were relatively modest. They did not suggest severe alterations in the NAC or other elements of SPNA circulation patterns.

While the analysis of variability in surface and subsurface thermohaline fields already suggests significant resilience of ocean circulation to the ongoing sea surface warming in the SPNA, direct evidence from ocean currents would substantiate this preliminary conclusion. To support this approach, we used geostrophic velocities derived from sea surface height (SSH) fields in SODA3 [35] and density data from WOA23 [47]. Notably, SSH data from SODA3 are available only for three decades: 1985–1994, 1995–2005, and 2005–2017. More details on the calculation of the current velocities can be found in [31]. A map of the winter velocity vectors at 50 m depth for the 1985–1994 decade is shown in Figure 6.

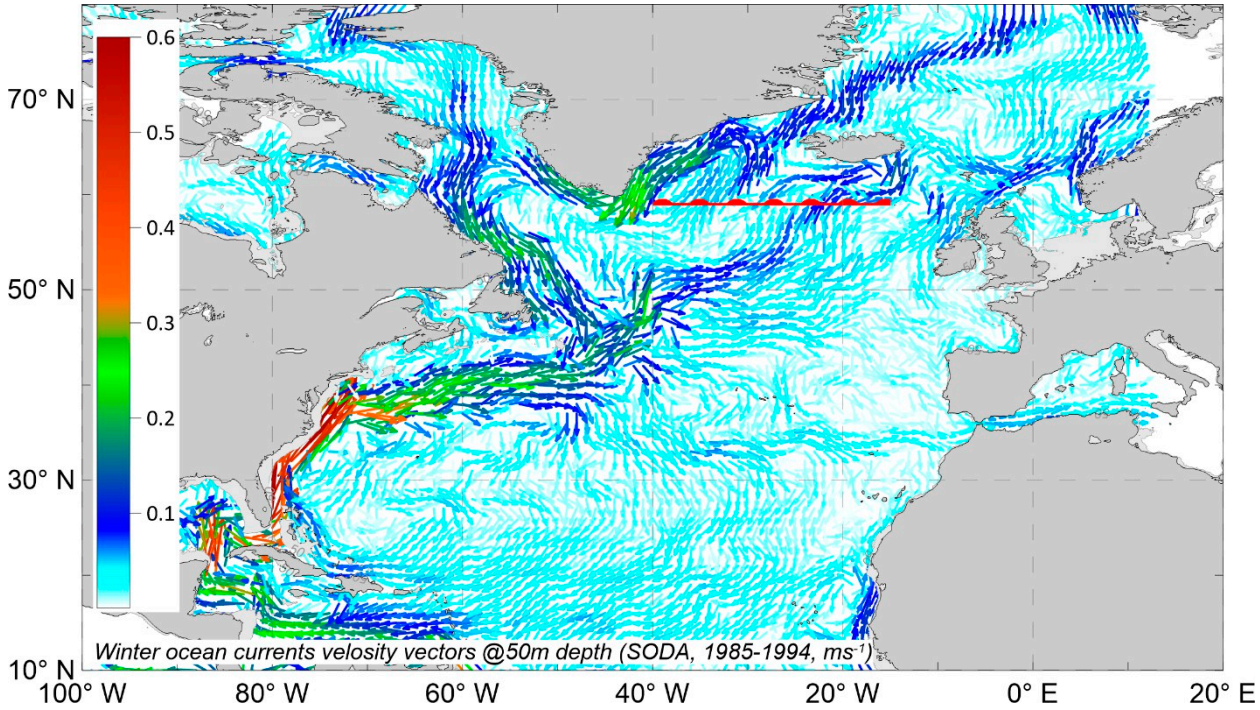

Figure 6. Winter velocity vectors for the 1985−1994 decade, computed using SSH from SODA3 and density from WOA23 at 50 m. The red line indicates the section from 40° W to 15° W, where the decadal section-averaged meridional velocity was calculated (see the text). The color bar units are ms^{-1}.

The northward component of the velocity vectors is of particular interest because the functionality of the AMOC primarily relies on it. Figure 7a illustrates the meridional (south-north) component of the velocity vector along a zonal section from 40° W to 15° W longitude at 59° N latitude (red line in Figure 6). The zonal section from 40° W to 15° W was selected based on the velocity structure to be as close to the NAC entering the Irminger Sea and NORS as possible. In a different section, the numbers would differ, but in our analysis, we used decadal *differences* in meridional velocity as a measure of AMOC change rather than absolute numbers.

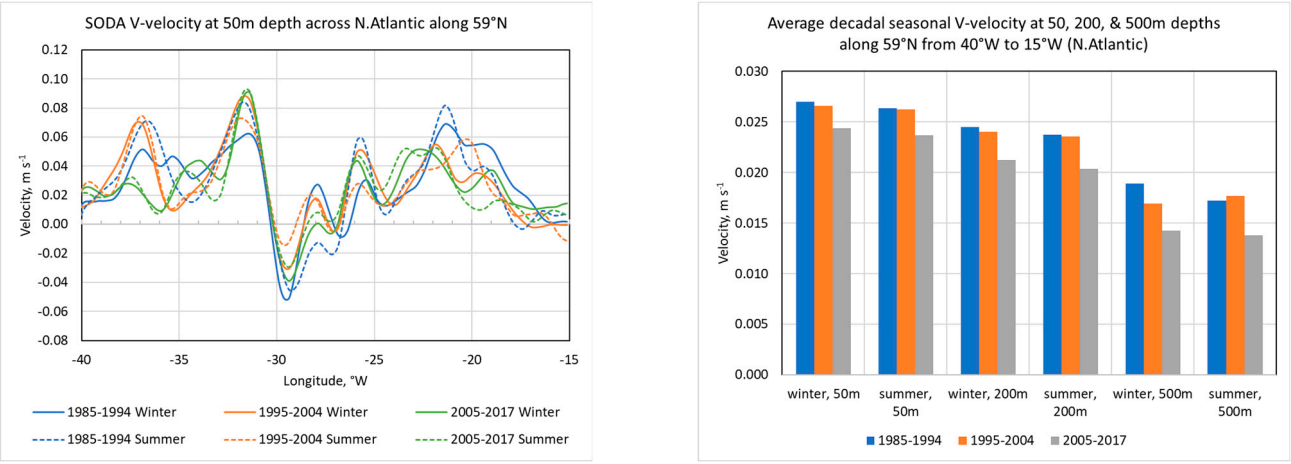

(**a**) (**b**)

Figure 7. Meridional (northward) components of the velocity vector at 50 m depth (**a**) and averaged meridional velocity component at 50 m, 200 m, and 500 m depths (**b**) for three decades in winter and summer. Based on the SODA3 analyses.

The AMOC's potential depends on the NAC transporting warm, salty water toward the eastern SPNA, where it exhibits the strongest northward velocity. We averaged the meridional component over that section for each decade at three depths (Figure 7b).

As illustrated in Figure 7b, the northward velocity diminished at all examined depths during both winter and summer, indicating a slight decline in the AMOC over the past three decades. Nevertheless, this decline should not be considered significant (e.g., at 50 m depth, changes in velocity over the last three decades were less than 10%). If this trend continues, a further decrease in the AMOC can be expected; however, the extent of this decline is unlikely to approach a collapse state.

To further elaborate on the findings highlighting the strong resilience of NA circulation, we used the SODA3 wind stress data to map the curl of the wind stress. These data spanned from 1980 to 2017. To complement the decadal climatologies from the WOA, we assembled three decadal wind-stress arrays and calculated the wind stress curl (WSC) for winter and summer seasons. Positive values of the wind stress curl indicate downward Ekman pumping, whereas negative values indicate upward Ekman pumping (also known as Ekman sucking).

Seidov et al. [11], building on their earlier research [31,48], contended that Ekman pumping is a crucial element and a potentially significant factor influencing AMOC stability. Notably, the two basin-wide circulation gyres, the subtropical and subpolar gyres, are divided by the zero line of the WSC (Figure 8a). The opposing directions of Ekman pumping are pivotal; warm water is pushed downward in the subtropical gyre, whereas cold water is drawn into the subpolar gyre.

The WSC analysis showed that the WSC zero line remained stable for at least 30 years, from 1985 to 2017 [11,31,48]. This is an essential feature of NA circulation during the ongoing warming of its sea surface, as documented by [39]. As surface waters continue to warm, Ekman pumping helps compensate by pumping additional heat downward in the subtropical gyre and sucking cold water up in the SPNA, thus supporting equilibrium and maintaining the stability of the subpolar front by preventing its northward drift.

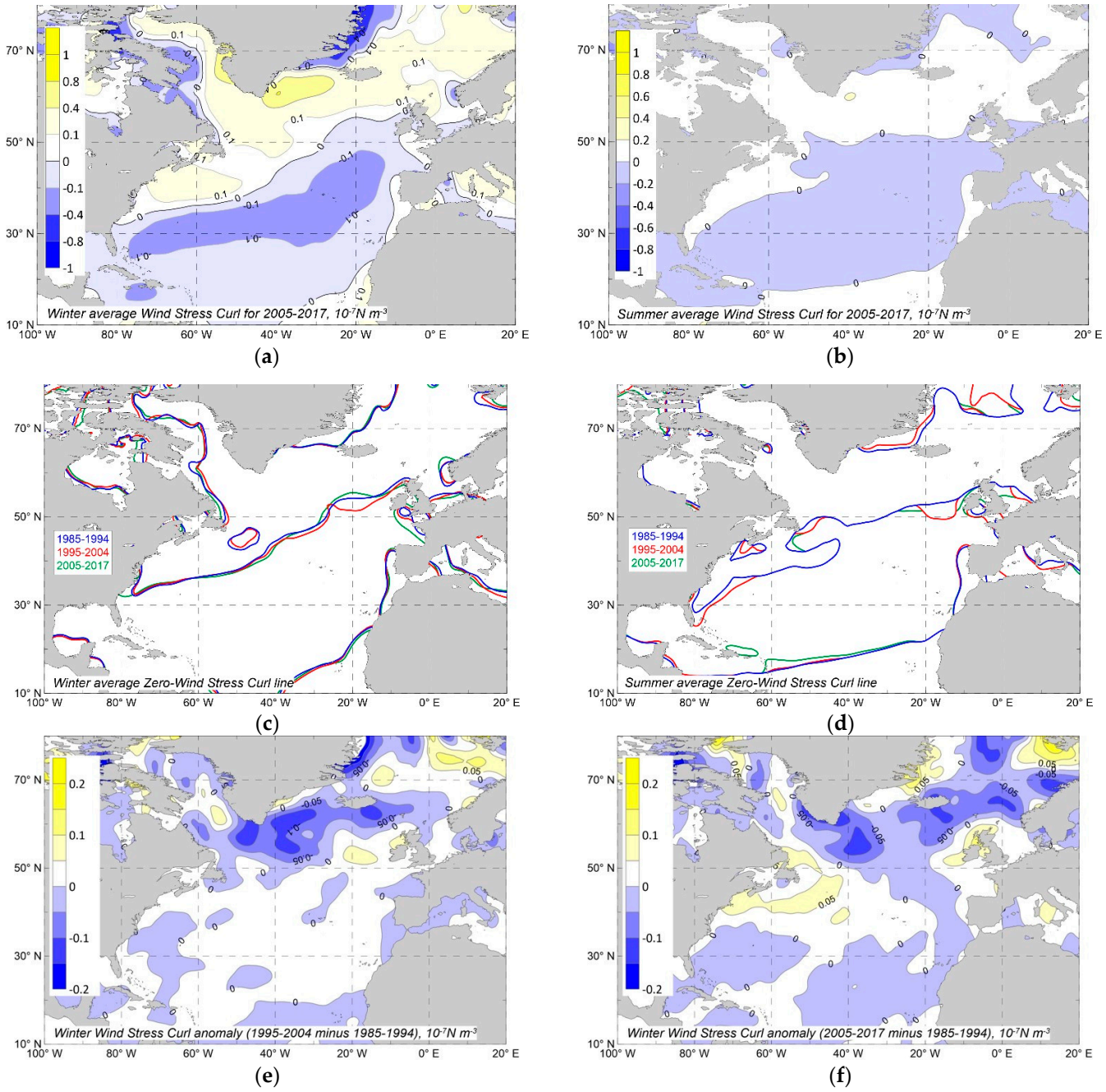

Figure 8. Winter (**a**) and summer (**b**) wind stress curl averaged from 1985 to 2017, and zero wind stress curl lines for three decades are shown in different colors for winter (**c**) and summer (**d**). The difference in the winter wind stress curl between the decades 1995–2004 and 1985–1994 (**e**) and between 2005–2017 and 1995–2004 (**f**). Based on the SODA3 analyses.

Figure 8 illustrates the WSC averaged over three decades from 1985 to 2017 for both winter (a) and summer (b). It also shows the decadal positions of the WSC zero line for these three decades in winter (c) and summer (d). Notably, although the position of the WSC zero line remained relatively stable over the years, seasonal variation was remarkable.

The overall NA dynamics can be associated with the WSC structure and the Ekman pumping geometry it induces, as discussed in previous publications [11,31]. Additionally, it has been suggested that Ekman pumping can affect the vertical structure of the AMOC and, consequently, its meridional coherence [49]. Figure 8e,f depict the variation in winter wind-stress curl between the decades 1995–2004 and 1985–1994 (Figure 8e) and 2005–2017 and 1995–2004 (Figure 8f), thus showing the progression of the WSC along the

NA climate trajectory. These differences indicate that the WSC has slightly strengthened in the subtropical gyres but weakened in most areas of the SPNA and NORS. This suggests that Ekman pumping intensifies downward in the subtropics and diminishes upward in the SPNA and NORS, thereby deepening the pycnocline. However, this deepening is far more pronounced in the eastern SPNA, especially in the NORS. Such differences in the heaving of the pycnocline can diminish isopycnal bending between the gyres and potentially counterbalance the stabilizing potential of the WSC geometry, that is, a stable zero line of the WSC preserving the gyres' geometry and the frontal boundary. Consequently, it can be argued that, in addition to a stable WSC geometry, a heaving thermocline can further preserve the gyre structure and polar front position. Although our analysis does not provide definitive proof, it is plausible that strengthening the pycnocline could help stabilize the AMOC, thereby counteracting the potentially increasing meltwater impact in the SPNA and NORS regions.

However, as shown in Figure 8a,e,f, the differences were small relative to the WOC average values (less than 10% in most areas). This suggests that the magnitude of the WSC impact is secondary to its geometry, which is defined by the zero line of the WSC. Without delving deeper into this theme, we believe that stable geometry and Ekman pumping could serve as potentially effective stabilizing mechanisms imposed by the WSC on NA circulation, at least partially accounting for its remarkable resilience despite ongoing surface warming over the past several decades.

5. Conclusions

Our arguments concerning the remarkable stability and resilience of the thermohaline structure in the SPNA and NORS, and consequently the upper arm of the AMOC, are based on the observed variability in temperature, salinity, density, velocity, and wind-stress fields on decadal timescales. However, these arguments should not be considered definitive for predicting the future AMOC behavior. Unanticipated abrupt changes can alter the AMOC's climatic trajectory, pushing it toward its tipping point. Nonetheless, we maintain that over the past 70 years, and particularly in the last 30 years, the thermohaline structures of the SPNA and NORS and their downstream impact on the AMOC have been remarkably stable and resilient.

This study continues our investigation of Gulf Stream resilience to ongoing surface warming [30]. In that publication, it was noted that the Gulf Stream, a crucial component of the upper arm of the AMOC, showed no significant changes over nearly 60 years. It was suggested that because the Gulf Stream dynamics largely determine the fate of the AMOC, the overall North Atlantic circulation remained stable during this period. However, at that time, we could not definitively claim this as a fact. In this extension and continuation of that study, through a comprehensive analysis of various parameters affecting the variability of the upper arm of the AMOC in the SPNA and NORS, we can now assert with much greater certainty that not only is the Gulf Stream but also the entire North Atlantic circulation stable and demonstrates a strong resilience to ongoing sea surface changes in this region. It should be noted that there is clear evidence of a gradual deceleration of the AMOC, albeit at a relatively slow rate. This means that, in the broadest sense, our analysis does not contradict the finding that the AMOC is undergoing a reduction phase. However, we contend that the overall climate trajectory in the NA is not as steep as it is sometimes portrayed and that developments over the past seven decades do not provide definitive indicators of an imminent AMOC collapse.

It is important to emphasize that, despite all indicators of the current stability and resilience of NA circulation, it remains uncertain whether a moderate slowing of the upper arm of the AMOC might lead to less stable and more vulnerable NA ocean climate patterns.

We cannot predict with certainty whether trends in sea surface temperature and density will accelerate towards significantly warmer and much less dense surface ocean waters in the foreseeable future. Global warming may accelerate faster than it currently does, potentially affecting AMOC dynamics. However, the available data are insufficient to predict these changes. Consequently, the future of the AMOC remains unclear. Nevertheless, our findings strongly suggest that the present-day NA ocean circulation and climate have remained stable over several decades despite observed surface warming. Therefore, based on our results, the collapse or severe damping of the AMOC appears to be unlikely in the near future.

Author Contributions: Conceptualization, D.S.; methodology, A.M. and J.R.; software, A.M. and J.R.; validation, D.S. and A.M.; formal analysis, D.S. and A.M.; investigation, D.S. and A.M.; resources, J.R.; data curation, A.M. and J.R.; writing—original draft preparation, D.S.; writing—review and editing, D.S., A.M., J.R.; visualization, A.M.; funding acquisition, A.M. and J.R. All authors have read and agreed to the published version of the manuscript.

Funding: This research was funded by NOAA Grants NA19NES4320002 and NA24NESX432C0001 (Cooperative Institute for Satellite Earth System Studies—CISESS) at the University of Maryland/ESSIC. Further support was provided by NOAA's Global Ocean Monitoring and Observing Program. The APC was funded by NOAA/NCEI.

Data Availability Statement: The data and maps based on the WOD, WOA, and SODA3 project that are used in this paper are publicly available at https://www.ncei.noaa.gov/products/world-ocean-atlas (accessed on 14 April 2026) and http://www.soda.umd.edu (accessed on 14 April 2026).

Acknowledgments: We want to thank the scientists, technicians, data center staff, and data managers for their contributions of data to the IOC/IODE, ICSU/World Data System, and NOAA/NCEI Ocean Archive System, which provided a foundation of in situ oceanographic data for our research that was used in this work. We thank our colleagues at NOAA/NCEI for many years of data processing and the construction of the World Ocean Database (WOD) and World Ocean Atlas (WOA). Dan Seidov, a former NOAA employee, recently retired. Despite this, he continued to list his affiliation with NOAA in his professional records because his work on this topic commenced before his retirement.

Conflicts of Interest: The authors declare no conflicts of interest. The views, opinions, and findings in this report are those of the authors and should not be construed as an official NOAA or US Government position, policy, or decision.

References

1. Buckley, M.W.; Marshall, J. Observations, inferences, and mechanisms of Atlantic Meridional Overturning Circulation variability: A review. *Rev. Geophys.* **2016**, *54*, 5–63. [CrossRef]
2. Weijer, W.; Cheng, W.; Drijfhout, S.S.; Fedorov, A.V.; Hu, A.; Jackson, L.C.; Liu, W.; McDonagh, E.L.; Mecking, J.V.; Zhang, J. Stability of the Atlantic Meridional Overturning Circulation: A Review and Synthesis. *J. Geophys. Res. Ocean.* **2019**, *124*, 5336–5375. [CrossRef]
3. Ditlevsen, P.; Ditlevsen, S. Warning of a forthcoming collapse of the Atlantic meridional overturning circulation. *Nat. Commun.* **2023**, *14*, 4254–4265. [CrossRef]
4. Vanderborght, E.; van Westen, R.M.; Dijkstra, H.A. Feedback Processes causing an AMOC Collapse in the Community Earth System Model. *J. Clim.* **2025**. [CrossRef]
5. van Westen, R.M.; Vanderborght, E.; Kliphuis, M.; Dijkstra, H.A. Physics-Based Indicators for the Onset of an AMOC Collapse Under Climate Change. *J. Geophys. Res. Ocean.* **2025**, *130*, e2025JC022651. [CrossRef]
6. Rahmstorf, S. Is the Atlantic Overturning Circulation approaching a tipping point? *Oceanography* **2024**, *37*, 16–29. [CrossRef]
7. Baker, J.A.; Bell, M.J.; Jackson, L.C.; Vallis, G.K.; Watson, A.J.; Wood, R.A. Continued Atlantic overturning circulation even under climate extremes. *Nature* **2025**, *638*, 987–994. [CrossRef]
8. Hu, A. Atlantic circulation could be more resilient to global warming than was thought. *Nature* **2025**, *638*, 893–894. [CrossRef] [PubMed]
9. Terhaar, J.; Vogt, L.; Foukal, N.P. Atlantic overturning inferred from air-sea heat fluxes indicates no decline since the 1960s. *Nat. Commun.* **2025**, *16*, 222. [CrossRef]

10. IPCC. *Climate Change 2021—The Physical Science Basis: Working Group I Contribution to the Sixth Assessment Report of the Intergovernmental Panel on Climate Change*; Cambridge University Press: Cambridge, UK, 2023.
11. Seidov, D.; Mishonov, A.; Reagan, J. AMOC and North Atlantic Ocean Decadal Variability: A Review. *Oceans* **2025**, *6*, 59. [CrossRef]
12. Sanchez-Franks, A.; Holliday, N.P.; Evans, D.G.; Fried, N.; Tooth, O.; Chafik, L.; Fu, Y.; Li, F.; de Jong, M.F.; Johnson, H.L. The Irminger Gyre as a key driver of the Subpolar North Atlantic Overturning. *Geophys. Res. Lett.* **2024**, *51*, e2024GL108457. [CrossRef]
13. Chafik, L.; Holliday, N.P.; Bacon, S.; Rossby, T. Irminger Sea Is the center of action for Subpolar AMOC Variability. *Geophys. Res. Lett.* **2022**, *49*, e2022GL099133. [CrossRef]
14. Reagan, J.R.; Seidov, D.; Wang, Z.; Dukhovskoy, D.; Boyer, T.P.; Locarnini, R.A.; Baranova, O.K.; Mishonov, A.V.; Garcia, H.E.; Bouchard, C.; et al. *World Ocean Atlas 2023, Volume 2: Salinity*; NOAA Atlas NESDIS 90; Mishonov, A., Ed.; NOAA/NESDIS: Silver Spring, MD, USA, 2024. [CrossRef]
15. Thornalley, D.J.R.; Oppo, D.W.; Ortega, P.; Robson, J.I.; Brierley, C.M.; Davis, R.; Hall, I.R.; Moffa-Sanchez, P.; Rose, N.L.; Spooner, P.T.; et al. Anomalously weak Labrador Sea convection and Atlantic overturning during the past 150 years. *Nature* **2018**, *556*, 227–230. [CrossRef]
16. Sicre, M.-A.; Hall, I.R.; Mignot, J.; Khodri, M.; Ezat, U.; Truong, M.-X.; Eiríksson, J.; Knudsen, K.-L. Sea surface temperature variability in the subpolar Atlantic over the last two millennia. *Paleoceanogr.* **2011**, *26*, PA4218. [CrossRef]
17. Marchal, O.; Waelbroeck, C.; Colin de Verdière, A. On the Movements of the North Atlantic Subpolar Front in the Preinstrumental Past. *J. Clim.* **2016**, *29*, 1545–1571. [CrossRef]
18. Keffer, T.; Martinson, D.G.; Corliss, B.H. The Position of the Gulf Stream During Quaternary Glaciations. *Science* **1988**, *241*, 440–442. [CrossRef]
19. Sarnthein, M.; Winn, K.; Jung, S.J.A.; Duplessy, J.C.; Labeyrie, L.; Erlenkeuser, H.; Ganssen, G. Changes in east Atlantic deepwater circulation over the last 30,000 years: Eight Time Slice Reconstructions. *Paleoceanography* **1994**, *9*, 209–267. [CrossRef]
20. Rahmstorf, S. Ocean circulation and climate during the past 120,000 years. *Nature* **2002**, *419*, 207–214. [CrossRef]
21. Liu, Z. Evolution of Atlantic Meridional Overturning Circulation since the last glaciation: Model simulations and relevance to present and future. *Philos. Trans. R. Soc. A Math. Phys. Eng. Sci.* **2023**, *381*, 20220190. [CrossRef] [PubMed]
22. Wharton, J.H.; Renoult, M.; Gebbie, G.; Keigwin, L.D.; Marchitto, T.M.; Maslin, M.A.; Oppo, D.W.; Thornalley, D.J.R. Deeper and stronger North Atlantic Gyre during the Last Glacial Maximum. *Nature* **2024**, *632*, 95–100. [CrossRef] [PubMed]
23. Seidov, D.; Sarnthein, M.; Stattegger, K.; Prien, R.; Weinelt, M. North Atlantic Ocean circulation during the last glacial maximum and subsequent meltwater event: A numerical model. *J. Geophys. Res. Ocean.* **1996**, *101*, 16305–16332. [CrossRef]
24. Ruddiman, W.F.; McIntyre, A. The North Atlantic Ocean during the last deglaciation. *Palaeogeogr. Palaeoclimatol. Palaeoecol.* **1981**, *35*, 145–214. [CrossRef]
25. CLIMAP. CLIMAP Project members: The surface of the ice-age Earth. *Science* **1976**, *191*, 1131–1137. [CrossRef]
26. Sarnthein, M.; Gersonde, R.; Niebler, S.; Pflaumann, U.; Spielhagen, R.; Thiede, J.; Wefer, G.; Weinelt, M. Overview of Glacial Atlantic Ocean Mapping (GLAMAP 2000). *Paleoceanography* **2003**, *18*, 1030. [CrossRef]
27. Pflaumann, U.; Sarnthein, M.; Chapman, M.; de Abreu, L.; Funnell, B.; Huels, M.; Kiefer, T.; Maslin, M.; Schulz, H.; Swallow, J.; et al. Glacial North Atlantic: Sea-surface conditions reconstructed by GLAMAP 2000. *Paleoceanography* **2003**, *18*, 1065. [CrossRef]
28. Eynaud, F.; de Abreu, L.; Voelker, A.; Schönfeld, J.; Salgueiro, E.; Turon, J.-L.; Penaud, A.; Toucanne, S.; Naughton, F.; Sánchez Goñi, M.F.; et al. Position of the Polar Front along the western Iberian margin during key cold episodes of the last 45 ka. *Geochem. Geophys. Geosyst.* **2009**, *10*, Q07U05. [CrossRef]
29. Zahn, R. Core correlations. *Nature* **1994**, *371*, 289–290. [CrossRef]
30. Seidov, D.; Mishonov, A.; Reagan, J.; Parsons, R. Resilience of the Gulf Stream path on decadal and longer timescales. *Sci. Rep.* **2019**, *9*, 11549. [CrossRef]
31. Mishonov, A.; Seidov, D.; Reagan, J. Revisiting the multidecadal variability of North Atlantic Ocean circulation and climate. *Front. Mar. Sci.* **2024**, *11*, 1345426. [CrossRef]
32. Mishonov, A.V.; Boyer, T.P.; Baranova, O.K.; Bouchard, C.N.; Cross, S.L.; Garcia, H.E.; Locarnini, R.A.; Paver, C.R.; Reagan, J.R.; Wang, Z. *World Ocean Database 2023*; NOAA Atlas NESDIS 97; NOAA/NESDIS: Silver Spring, MD, USA, 2024. [CrossRef]
33. Locarnini, R.A.; Mishonov, A.V.; Baranova, O.K.; Reagan, J.R.; Boyer, T.P.; Seidov, D.; Wang, Z.; Garcia, H.E.; Bouchard, C.; Cross, S.L.; et al. *World Ocean Atlas 2023, Volume 1: Temperature*; NOAA Atlas NESDIS 89; NOAA/NESDIS: Silver Spring, MD, USA, 2024; p. 52. [CrossRef]
34. Schlitzer, R. Ocean Data View. Available online: https://odv.awi.de (accessed on 10 April 2026).
35. Carton, J.A.; Chepurin, G.A.; Chen, L. SODA3: A new ocean climate reanalysis. *J. Clim.* **2018**, *31*, 6967–6983. [CrossRef]
36. Bryden, H.L.; Longworth, H.R.; Cunningham, S.A. Slowing of the Atlantic meridional overturning circulation at 25°N. *Nature* **2005**, *438*, 655–657. [CrossRef]
37. Rahmstorf, S.; Box, J.E.; Feulner, G.; Mann, M.E.; Robinson, A.; Rutherford, S.; Schaffernicht, E.J. Exceptional twentieth-century slowdown in Atlantic Ocean overturning circulation. *Nat. Clim. Change* **2015**, *5*, 475–480. [CrossRef]

38. Caesar, L.; Rahmstorf, S.; Robinson, A.; Feulner, G.; Saba, V. Observed fingerprint of a weakening Atlantic Ocean overturning circulation. *Nature* **2018**, *556*, 191–196. [CrossRef]
39. Levitus, S.; Antonov, J.I.; Boyer, T.P.; Baranova, O.K.; Garcia, H.E.; Locarnini, R.A.; Mishonov, A.V.; Reagan, J.R.; Seidov, D.; Yarosh, E.S.; et al. World Ocean heat content and thermosteric sea level change (0–2000 m), 1955–2010. *Geophys. Res. Lett.* **2012**, *39*, L10603. [CrossRef]
40. Zhu, C.; Liu, Z. Weakening Atlantic overturning circulation causes South Atlantic salinity pile-up. *Nat. Clim. Change* **2020**, *10*, 998–1003. [CrossRef]
41. Li, K.-Y.; Liu, W. Weakened Atlantic Meridional Overturning Circulation causes the historical North Atlantic Warming Hole. *Commun. Earth Environ.* **2025**, *6*, 416. [CrossRef]
42. Molodtsov, S.; Marinov, I.; Weijer, W.; DeSantis, D.; Jonko, A.; Veneziani, M.; Lu, J. North Atlantic temperature and salinity changes are driven by external forcing, underestimated by CMIP6 models. *npj Clim. Atmos. Sci.* **2025**, *8*, 332. [CrossRef]
43. Seidov, D.; Mishonov, A.; Reagan, J.; Parsons, R. Multidecadal variability and climate shift in the North Atlantic Ocean. *Geophys. Res. Lett.* **2017**, *44*, 4985–4993. [CrossRef]
44. Pollard, R.T.; Read, J.F.; Holliday, N.P.; Leach, H. Water masses and circulation pathways through the Iceland Basin during Vivaldi 1996. *J. Geophys. Res.* **2004**, *109*, C04004. [CrossRef]
45. Dickson, R.R.; Brown, J. The Production of North Atlantic Deep Water—Sources, Rates, and Pathways. *J. Geophys. Res. Ocean.* **1994**, *99*, 12319–12341. [CrossRef]
46. Sarnthein, M.; Blaser, P. Peak glacial-to-Heinrich-1 changes in Denmark Strait Overflow and seawater stratification in the Nordic Seas, a switchboard of changes in Atlantic Meridional Overturning Circulation and the 'Nordic Heat Pump'. *Quat. Sci. Rev.* **2025**, *355*, 109181. [CrossRef]
47. Reagan, J.R.; Garcia, H.E.; Boyer, T.P.; Baranova, O.K.; Bouchard, C.; Cross, S.L.; Dukhovskoy, D.; Grodsky, A.; Locarnini, R.A.; Mishonov, A.V. *World Ocean Atlas 2023: Product Documentation*; NOAA/NESDIS: Silver Spring, MD, USA, 2024. [CrossRef]
48. Seidov, D.; Mishonov, A.; Reagan, J.; Parsons, R. Eddy-resolving in situ ocean climatologies of temperature and salinity in the Northwest Atlantic Ocean. *J. Geophys. Res. Ocean.* **2019**, *124*, 41–58. [CrossRef]
49. Fraser, N.J.; Fox, A.D.; Cunningham, S.A. Impact of Ekman pumping on the meridional coherence of the AMOC. *Geophys. Res. Lett.* **2025**, *52*, e2024GL108846. [CrossRef]